Design of Frequency Selective Surface Structure With High Angular Stability for Radome Application

Ning Liu, Xianjun Sheng, Chunbo Zhang, and Dongming Guo

***Abstract*—A design method for frequency selective surface (FSS) structure with high angular stability has been proposed in this letter. In the proposed method, bandwidth angular stability of FSS structure has been improved by adopting the bandwidth compensation technique, and structural parameters can be obtained with a curve-fitting method from the desired resonate frequency and bandwidth. Discussions on improving the bandwidth design accuracy have been presented. By taking bandwidth angular stability into consideration, the structure designed by the proposed method is more suitable to construct FSS radome. For verification, an FSS structure operating at 15 GHz with a bandwidth of 2 GHz has been designed, fabricated, and measured. Good agreements between the simulated and measured results can be observed.**

***Index Terms*—Angular stability, equivalent circuit model (ECM), frequency selective surface (FSS), radome.**

I. Introduction

AIRBORNE radomes are placed in front of the airborne radar system to protect microwave components from the damage due to outer extreme environment [1]. Recently, with the development of military system, aircrafts with lower radar cross section (RCS) are highly desired. For the purpose of RCS reduction, frequency selective surface (FSS) radomes have been proposed and investigated [2]. Typically, FSS radomes are composed of one or more FSS layers embedded in dielectric substrates. As a result, FSS radome is transparent to the working frequency and is opaque to the frequency out of the frequency band, which shows a frequency filtering property. Hence, FSS radome is an ideal candidate for low-observable aircraft design. Meanwhile, for the purpose of RCS reduction, frequency filtering property of FSS radome should be stable at oblique incidence with larger incident angle.

To design an ideal FSS radome for RCS reduction, different structures have been proposed. A frequency selective radome with wideband absorbing characteristic was proposed in [3]. Composite sandwich structures are adopted to construct low-observable radomes in [4] and [5]. A miniature conical thickness FSS radome is designed in [6], and in [7] a dual-layer FSS radome is proposed. Absorptive FSS has been adopted to construct radome to realize an out-of-band absorbing characteristic in [8]. Most of the research focuses on novel structure design rather than methods for synthesizing FSS radome according to the desired frequency response.

As for the synthesis problem, binary particle swarm optimization algorithm combined with pixel-overlap technique has been proposed in [9] to design FSS radome. Method for designing FSS has also been proposed in [10]. However, bandwidth (BW) angular stability of FSS radome has not been taken into consideration in this research. Meanwhile, due to the lacking of discussions on the effect of dielectric substrate on frequency filtering property, method in [10] is not suitable for FSS radome design.

In this letter, we propose a synthesis method for FSS structure to construct the radome wall. Compared with the method in [10], the proposed method takes both the BW angular stability and the influence of core dielectric substrate into consideration. Although the BW angular stability in the method is achieved with the technique in [11], the proposed method solves the synthesis problem of the FSS structure and adds discussions on improving the design accuracy. Hence, the proposed method is more suitable for FSS radome design.

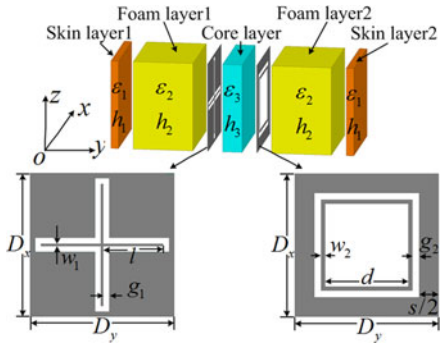

Fig. 1. Geometrical configuration of the proposed FSS structure.

II. Proposed Design Method

As shown in Fig. 1, the proposed FSS structure is composed of two FSS layers embedded in five dielectric substrates, which is suitable to construct FSS radome. The top FSS layer is composed of gridded square loop element, and the bottom one consists of

Manuscript received October 17, 2017; revised November 23, 2017; accepted November 24, 2017. Date of publication November 28, 2017; date of current version January 10, 2018. This work was supported in part by the National Natural Science Foundation of China under Grant 51575081 and in part by the Fundamental Research Funds for the Central Universities of China under Grant DUT17ZD304. *(Corresponding author: Xianjun Sheng.)*

N. Liu and D. Guo are with the School of Mechanical Engineering, Dalian University of Technology, Dalian 116024, China (e-mail: liuning@mail.dlut.edu.cn; guodm@dlut.edu.cn).

X. Sheng is with the School of Electrical Engineering, Dalian University of Technology, Dalian 116024, China (e-mail: sxianjun@dlut.edu.cn).

C. Zhang is with the Research Institute of Aerospace Special Materials and Processing Technology, Beijing 100071, China (e-mail: 950869@qq.com).

Digital Object Identifier 10.1109/LAWP.2017.2778078

1536-1225 © 2017 IEEE. Personal use is permitted, but republication/redistribution requires IEEE permission.
See http://www.ieee.org/publications_standards/publications/rights/index.html for more information.

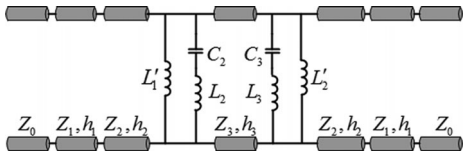

Fig. 2. Equivalent circuit model of the proposed FSS structure.

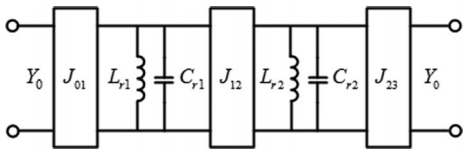

Fig. 3. Equivalent circuit model of the second-order bandpass filter using shunt *LC* resonators and *J*-inverters.

cross-loop aperture element. The two FSS layers are separated by the core material layer for coupling. Skin material layer and foam material layer are bonded outside the FSS layers for the purpose of BW compensation.

Based on the equivalent circuit theory, frequency filtering property of the proposed FSS structure can be predicted via its equivalent circuit model (ECM). Considering the frequency response of the two FSS layers, they both can be depicted by the parallel of an inductor and a series *LC* resonator. The dielectric layers can be modeled by short transmission lines. Hence, the proposed structure can be described by the ECM in Fig. 2. In which L_1' and $L_2 - C_2$ are the equivalent circuit parameters of the gridded square loop element and L_2' and $L_3 - C_3$ are the parameters of the cross-loop aperture element.

In order to obtain the structural parameters of the FSS structure from the desired frequency filtering property, equivalent circuit parameters in Fig. 2 should be first determined. Motivated by this requirement, ECM of the second-order bandpass filter in Fig. 3 is adopted. Based on the filter theory, equivalent circuit parameters of the second-order filter can be calculated from the desired resonant frequency f_0 and –3 dB bandwidth (BW). Once the equivalent circuit parameters in Fig. 3 are obtained, we can map these equivalent circuit parameters to the equivalent circuit parameters in Fig. 2 based on the discussions in [10]. The mapped equivalent circuit parameters can be obtained by

$$L_i' = \frac{1 - (f_0/f_{zi})^2}{(2\pi f_0)^2 C_{i+1}}, \quad i = 1, 2 \tag{1}$$

$$C_{i+1} = C_{ri}\left(1 - (f_0/f_{zi})^2\right)^2, \quad i = 1, 2 \tag{2}$$

$$L_{i+1} = \frac{1}{(2\pi f_{zi})^2 C_{i+1}}, \quad i = 1, 2 \tag{3}$$

with

$$C_{r1} = \frac{J_{01}^2 g_0 g_1 Z_0}{2\pi \mathrm{BW}} = 1/(2\pi f_0)^2 L_{r1} \tag{4}$$

$$C_{r2} = \frac{J_{23}^2 g_2 g_3 Z_0}{2\pi \mathrm{BW}} = 1/(2\pi f_0)^2 L_{r2} \tag{5}$$

$$J_{01} = J_{23} = \sqrt{\varepsilon_2}/Z_0 \tag{6}$$

where g_i $(i = 0, 1, 2, 3)$ are the element values for a low-pass filter prototype. f_{zi} $(i = 1, 2)$ are the resonant frequencies of the transmission zeroes produced by the two FSS layers. Z_0 is the wave impedance in free.

Subsequently, thicknesses of dielectric layers h_i $(i = 1, 2, 3)$ should be determined. Thicknesses of the outer dielectric layers can be determined by the BW compensation technique proposed in [11], and the thickness of the core dielectric substrate can be determined by considering the coupling effect between FSS layers. Hence, as proposed in [11], skin layer thickness h_1 and foam layer thickness h_2 can be determined by

$$h_1 = \frac{0.25 \cdot \lambda_0 \cdot [(1 + \cos\theta_{\max}) - \varepsilon_2]}{(\varepsilon_1 - \varepsilon_2) \cdot \sqrt{1 + \cos\theta_{\max}}} \tag{7}$$

$$h_2 = \frac{0.25 \cdot \lambda_0 \cdot [\varepsilon_1 - (1 + \cos\theta_{\max})]}{(\varepsilon_1 - \varepsilon_2) \cdot \sqrt{1 + \cos\theta_{\max}}} \tag{8}$$

where λ_0 is the wavelength in free space, ε_1 is the relative permittivity of the skin material, ε_2 is the relative permittivity of the foam material, and $\theta_{\max}$ is the largest incident angle considered in the FSS radome design. Also, considering the coupling effect between the two FSS layers, core layer thickness h_3 can be calculated by

$$h_3 = 0.25\ \lambda_0/\sqrt{\varepsilon_3} \tag{9}$$

where ε_3 is the relative permittivity of the core material.

After determining the thicknesses of the dielectric layers and the equivalent circuit parameters, the desired transmission coefficient curve can be calculated via the ECM in Fig. 2 by the transmission line equations. Then, FSS structural parameters can be extracted from the desired transmission coefficient curve with a curve fitting method. In which, particle swarm optimization (PSO) algorithm [12] has been adopted to obtain the optimized structural parameters. To promote the evaluation of the particle swarm, a fitness function has been defined as follows:

$$\mathrm{Fit} = \sqrt{\frac{1}{N}\sum_{i=1}^{N}\left(S_{\mathrm{com}}(f_i) - S_{\mathrm{des}}(f_i)\right)^2} \tag{10}$$

where *N* is the total number of calculated frequency, $S_{\mathrm{com}}(f_i)$ is the simulated transmission coefficient at f_i of each particle, and $S_{\mathrm{des}}(f_i)$ is the desired transmission coefficient calculated by the ECM in Fig. 2. Obviously, the smaller the fitness value is, the better the FSS structural parameters are. To summarize the proposed method, a flowchart is given in Fig. 4.

III. Verification of the Proposed Method

To verify the validity of the proposed method, an FSS has been designed with the structure shown in Fig. 1. It is desired that the FSS can provide a passband operating at $f_0 = 15$ GHz with a –3 dB BW of $\mathrm{BW} = 2$ GHz. There are two transmission zeros operating at $f_{z1} = 18$ GHz and $f_{z2} = 22.5$ GHz, respectively. Also, frequency filtering property of the FSS should be stable within incident angle of $\theta_{\max} = 60^\circ$. Considering the manufacturability of the FSS, engineering available materials have been adopted to construct the dielectric substrates. Relative permittivity and tangent loss of the skin material are set to be $\varepsilon_1 = 3.15$ and $tg\delta_1 = 0.015$, relative permittivity

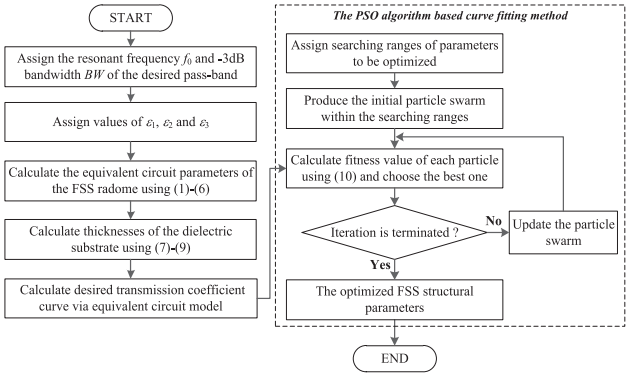

Fig. 4. Flowchart of the proposed design method.

and tangent loss of the foam material are $\varepsilon_2 = 1.1$ and $tg\delta_2 = 0.005$, and the core material is with a relative permittivity of $\varepsilon_3 = 2.3$ and a tangent loss of $tg\delta_3 = 0.003$.

In order to obtain the flat-top characteristic in the passband, Butterworth low-pass filter prototype has been chosen, and the element values are set to be $g_0 = 1$, $g_1 = 1.414$, $g_2 = 1.414$, $g_3 = 1$. Then, equivalent circuit parameters can be calculated with (1)–(6) as follows: $L_1' = 1.122$ nH, $L_2 = 2.551$ nH, $C_2 = 0.031$ pF, $L_2' = 0.617$ nH, $L_3 = 0.494$ nH, and $C_3 = 0.1$ pF. By using (7)–(9), thicknesses of the dielectric layers are calculated to be $h_1 = 0.79$ mm, $h_2 = 3.29$ mm, and $h_3 = 3.297$ mm. Dielectric substrates with the calculated thicknesses may by not available in engineering. Thicknesses of the dielectric layers are set to be $h_1 = 0.8$ mm, $h_2 = 3.3$ mm, and $h_3 = 3.3$ mm.

After acquiring the equivalent circuit parameters and the thicknesses of dielectric layers, the desired transmission coefficient curve can be calculated with the ECM in Fig. 2. Then, structural parameters of the FSS structure can be extracted from the desired transmission coefficient curve using a PSO-algorithm-based curve fitting method. In the PSO algorithm, FSS structural parameters are chosen as the parameters to be optimized, and searching ranges are set to be: 3 mm $\leq D_x = D_y \leq$ 10 mm, 2 mm $\leq d \leq$ 8 mm, 1 mm $\leq l \leq$ 6 mm, 0.05 mm $\leq w_1 \leq$ 2 mm, 0.1 mm $\leq g_1 \leq$ 2 mm, 0.05 mm $\leq w_2 \leq$ 2 mm, 0.1 mm $\leq g_2 \leq$ 4 mm. Noting that, other structural parameters can be obtained with geometrical operations. Also, population of the particle swarm is set to be 40, and values of the two acceleration constants are set to be $c_1 = 2.0$ and $c_2 = 2.4$. With the PSO algorithm, the optimized parameters are as follows: $D_x = D_y = 6$ mm, $l = 2.5$ mm, $w_1 = 0.1$ mm, $g_1 = 0.25$ mm, $d = 3.5$ mm, $w_2 = 0.15$ mm, $g_2 = 0.3$ mm, $s = 1.6$ mm.

Once structural parameters of the FSS structure are obtained, performance of the designed FSS can be investigated by both full-wave simulations and experimental verifications. As shown in Fig. 5, an FSS prototype has been fabricated. The two FSS layers are fabricated on the core substrate with the standard printed-circuit-board process technology, and the skin layers together with the foam layers are bounded outside the FSS layers. The FSS layers are composed of 83 × 83 elements, and the overall size of the prototype is about 500 × 500 mm. Transmission coefficient of the FSS is measured in a microwave anechoic chamber with the free-space measurement system, which

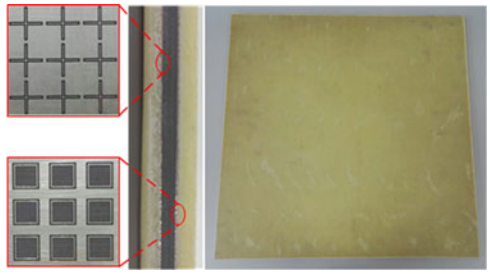

Fig. 5. Photograph of the fabricated FSS.

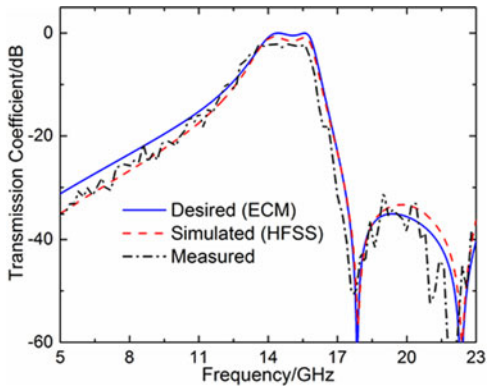

Fig. 6. Transmission coefficients obtained by different methods.

TABLE I
COMPARISONS BETWEEN THE SIMULATED AND MEASURED RESULTS

	f_0 (GHz)	f_{Z1} (GHz)	f_{Z2} (GHz)	–3 dB BW (GHz)
Desired	15	18	22.5	2
Simulated (ECM)	15.05	17.86	22.44	2.16
Simulated (CST)	15.02	17.89	22.39	2.12
Measured	14.8	17.8	22.2	2.18

is mainly composed of two horn antennas, a vector network analyzer and a turntable. The fabricated FSS is placed on the turntable to control the incident angle, and the turntable is placed between the two horn antennas with a distance of 3 m and 0.5 m, respectively. The measurement can be carried out into two steps to ensure the accuracy: 1) The transmission coefficient is measured without the FSS prototype. 2) The transmission coefficient with the FSS prototype is measured. Then, the transmission coefficients measured in step 2) are calibrated with the results in step 1).

The measured transmission coefficient at normal incidence together with the simulated results obtained by ECM and full-wave simulation software HFSS are shown in Fig. 6. Meanwhile, comparisons between the results obtained by these three methods have been carried out and shown in Table I. As indicated by Fig. 1 and Table I, good agreements between the three methods can be observed, which demonstrates the validity of the proposed method. However, compared with the desired values of the resonant frequency and BW, deviations of the simulated and measured results are about 10%. Although these

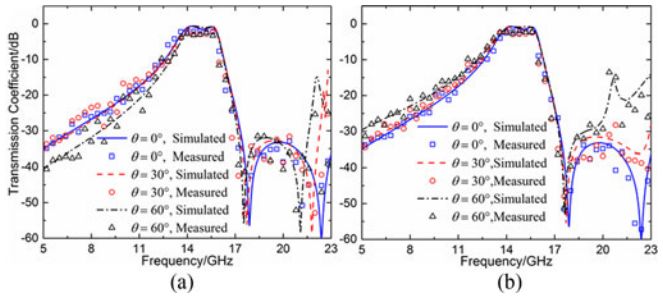

Fig. 7. Comparisons between the simulated and the measured results. (a) For TE polarization. (b) For TM polarization.

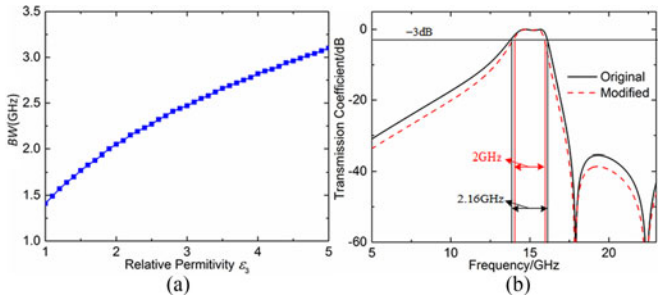

Fig. 8. (a) Influence of relative permittivity ε_3 on BW. (b) Comparisons between the transmission coefficients with and without the modification strategy.

deviations are acceptable, modifications of the proposed method should be discussed to improve the design accuracy. It is noted that insertion losses of the transmission coefficients obtained by full-wave simulations and experimental verification are larger than that obtained by the equivalent circuit model. This discrepancy is mainly caused by dielectric loss of substrate layers and ohmic loss of FSS layers. Meanwhile, ripples in the measured result are mainly caused by the edge diffraction of the FSS prototype.

Finally, transmission coefficients under oblique incidence with different polarizations have been measured to investigate the angular stability of the designed FSS. The measured results along with the simulated ones obtained by HFSS are shown in Fig. 7. As observed, frequency filtering property of the designed FSS maintains well at oblique incidence of 60°. Especially, the flat-top characteristic in the passband remains unchanged for both TE and TM polarizations at oblique incidence, which is important for an ideal FSS radome design. Also, to depict the BW angular stability, the ratio of BW at oblique incidence and BW at normal incidence has been taken into consideration. Simulated results show that BW ratio at 60° of the designed FSS is only 0.98 and 1.017 for TE and TM polarization, respectively.

In order to improve the BW design accuracy of the proposed method, numerical simulations have been carried out to investigate the influence of relative permittivity of core material on BW. In the simulations, relative permittivity ε_3 is ranging from 1 to 5 with a step of 0.1. Then, transmission coefficient of the FSS structure can be obtained with the equivalent circuit model, and corresponding BWs for each value of ε_3 can be calculated. As shown in Fig. 8(a), it can be found that –3 dB BW obtained with the proposed equivalent circuit model shown in Fig. 2 is related to the relative permittivity of the core material ε_3. The larger value of ε_3 leads to larger value of BW. This relationship will lead to the BW design error of the proposed method, which can be observed from Table I. We can compensate this error with the following strategy: 1) Assign the desired BW and calculate the transmission coefficient with the equivalent circuit model, then we can obtain the calculated BW BW_C. 2) Modify the desired value of BW with the deviation value between BW and BW_C. As shown in Fig. 8(b), with this compensation strategy, the deviation of BW between calculated and designed values can be eliminated. It should point out that the deviation value between BW and BW_C is obtained with the equivalent circuit model. Hence, the modification strategy is not time-consuming.

IV. Conclusion

A design method for synthesizing FSS with stable frequency response has been proposed. The proposed method solves the problem of acquiring structural parameters from the desired frequency filtering property. Also, by adopting BW compensation technique, FSS structure designed with the proposed method can provide stable frequency filtering property with respect to both incident angles and polarizations. For verification, an FSS has been designed, fabricated, and measured. Both simulated and measured results demonstrate the validity of the proposed method. The proposed design method can be applied to synthesize FSS radome in the field of microwave and communication.

References

[1] D. J. Kozakoff, *Analysis of Radome-Enclosed Antennas*. Norwood, MA, USA: Artech House, 1997.

[2] E. Martini, F. Caminita, M. Nannetti, and S. Maci, "Fast analysis of FSS radome for antenna RCS reduction," in *Proc. IEEE Int. Symp. Antennas Propag. Soc.*, Jul. 2006, pp. 1801–1804.

[3] F. Costa and A. Monorchio, "A frequency selective radome with wideband absorbing properties," *IEEE Trans. Antennas Propag.*, vol. 60, no. 6, pp. 2740–2747, Jun. 2012.

[4] P. C. Kim, D. G. Lee, I. S. Seo, and G. H. Kim, "Low-observable radomes composed of composite sandwich constructions and frequency selective surfaces," *Composites Sci. Technol.*, vol. 68, no. 9, pp. 2163–2170, 2008.

[5] I. Choi, J. G. Kin, and I. S. Seo, "Aramid/epoxy composites sandwich structures for low-observable radomes," *Composites Sci. Technol.*, vol. 71, no. 14, pp. 1632–1638, 2011.

[6] B. Q. Lin, F. Li, Q. R. Zheng, and Y. S. Zen, "Design and simulation of a miniature thick-screen frequency selective surface radome," *IEEE Antennas Wireless Propag. Lett.*, vol. 8, pp. 1065–1068, 2009.

[7] H. Chen, X. Hou, and L. Deng, "Design of frequency selective surfaces radome for a planar slotted waveguide antenna," *IEEE Antennas Wireless Propag. Lett.*, vol. 8, pp. 1231–1233, 2009.

[8] Q. Cheng and Y. Q. Fu, "A plannar stealthy antenna radome using absorptive frequency selective surface," *Microw. Opt. Technol. Lett.*, vol. 56, no. 8, pp. 1788–1792, 2014.

[9] N. Liu, X. J. Sheng, C. B. Zhang, J. J. Fan, and D. M. Guo, "Design of FSS radome using binary particle swarm algorithm combined with pixel-overlap technique," *J. Electromagn. Waves Appl.*, vol. 5, pp. 522–531, 2017.

[10] B. Li and Z. Shen, "Synthesis of quasi-elliptic bandpass frequency selective surface using cascaded loop arrays," *IEEE Trans. Antennas Propag.*, vol. 61, no. 6, pp. 3053–3059, Jun. 2013.

[11] N. Liu, X. J. Sheng, C. B. Zhang, J. J. Fan, and D. M. Guo, "A feasible bandwidth compensation technique for FSS radome design," *IEICE Electron. Express*, vol. 14, no. 13, 2017, Art. no. 20170510.

[12] J. Kennedy and R. C. Eberhart, "Particle swarm optimization," in *Proc. IEEE Int. Conf. Neural Netw.* Perth, Australia, 1995, vol. IV, pp. 1942–1948.